Chapter 3

MRI artifacts in human brain tissue after prolonged formalin storage

Adapted from Magn Reson Med. 2011 Jun;65(6):1750-8

Rob J.A. Nabuurs[#1]
Sara van Duijn[#2]
Sanneke van Rooden[1]
Marion L.C. Maat-Schieman[3]
Sjoerd G. van Duinen[2]
Mark A. van Buchem[1]
Louise van der Weerd[1,4]
Remco Natté[2]

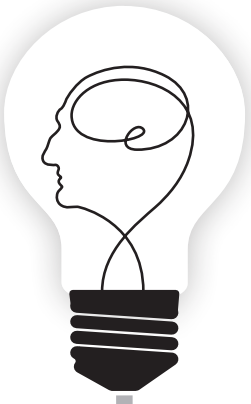

Abstract

For the interpretation of magnetic resonance imaging (MRI) abnormalities in brain pathology, often *ex vivo* tissue is used. The purpose of the present study was to determine the pathological substrate of several distinct forms of MR hypo-intensities that were found in formalin-fixed brain tissue with amyloid-β (Aβ) deposits. Samples of brain cortex were scanned using T_2*-weighted protocols at several resolutions on a 9.4T MRI scanner. High resolution MRI showed large coarse hypo-intensities throughout the cortical gray and white matter, corresponding to macroscopic discolorations and microscopic circumscribed areas of granular basophilic neuropil changes, without any further specific tissue reactions or Aβ related pathology. These coarse MRI hypo-intensities were identified as localized areas of absent neuropil replaced by membrane/myelin sheath remnants using electron microscopy. Interestingly, the presence/absence of these tissue alterations was not related to amyloid deposits, but strongly correlated to the fixation time of the samples in unrefreshed formalin. These findings show that prolonged storage of formalin fixed brain tissue results in subtle histology artifacts which show on MRI as hypo-intensities that on first appearance are indistinguishable from genuine brain pathology. This indicates that post-mortem MRI should be interpreted with caution, especially if the history of tissue preservation is not fully known.

Introduction

MR imaging of post-mortem brain tissue offers a valuable research method to study disease related changes in image contrast, because the findings can be correlated to histology.[1-12] High resolution *ex vivo* imaging has been a useful tool in interpreting the MRI features of many neurodegenerative disorders, including multiple sclerosis (MS), Alzheimer's disease (AD), and (sporadic) cerebral amyloid angiopathy.[1-3,6-9,11,12] However, the MR characteristics of the tissue rapidly change in the post-mortem situation due to tissue decomposition and chemical fixation; therefore direct translation of the findings to the clinical setting has to be done with caution.[13-19] Firstly, tissue decomposition occurs during the post-mortem interval (PMI), the time period between the patient's somatic death and beginning of the immersion-fixation of the tissue, which varies among subjects. Several studies have shown that an increasing PMI leads to a reduction of T_1 and T_2.[13,15,20] A more recent study, however, suggested these findings might mainly be due to tissue dehydration or the fixative itself. When these effects were minimized, proton density, T_1 and T_2 values all increased with longer PMI.[17] Also mean diffusivity and fractional anisotropy decrease with prolonged PMI.[17,21]
After autopsy, brain tissue will be immersed into a solution containing a chemical fixative, most frequently being formalin also known as formaldehyde. These solutions preserve tissue by slowly diffusing into it, leading to the cross-linking of proteins and immobilization of water molecules, thereby preventing autolysis and tissue decomposition.[21-23] By its nature it is to be expected that this would affect MR characteristics, which indeed was confirmed by several post-mortem brain MRI studies. A reverse in gray matter (GM) / white matter (WM) T_1 contrast occurs within several days of fixation, merely due to a rapid decline in the latter combined with a general decrease in both continuing at least up to three months.[18] Similarly, T_2 relaxation declines with prolonged fixation affecting both GM and WM, reaching a stable plateau as shown by consecutively imaging up to six months fixation.[13-15,18]

All of the above has led to important considerations on the correct method to obtain and interpret post-mortem MR images.[13,15]
However, similar studies investigating the effect of long fixation periods (> 6 months) on the MR characteristics have not yet been published. Nevertheless, this question is important, especially when using rare material from tissue archives, which are stored using fixatives like formalin for periods ranging from several years up to decades. In a recent study using archival tissue with prolonged fixation times, we noticed unusually large coarse hypo-intensities, especially apparent on high resolution T_2*-weighted images, in several brain samples regardless their pathological diagnosis. We hypothesized that these coarse hypo-intensities were the result of the extended formalin fixation period.
The purpose of the current study therefore was to investigate the occurrence of these T_2* changes with respect to their formalin fixation time in brain samples with different pathologies. To this end, MR images were obtained of eighteen samples with fixation times ranging from 3 months to several decades. Subsequently the samples were evaluated both macroscopically and microscopically to identify the occurrence and the microscopic substrate of tissue changes due to prolonged fixation.

Materials and Methods

Subjects

We used brain tissue of six patients with AD, four patients with Hereditary Cerebral Hemorrhage with Amyloidosis, Dutch type (HCHWA-D), two patients with Down's Syndrome (DS), two patients with sporadic Cerebral Amyloid Angiopathy (CAA) and four control brains. (**Table 3.1**) The brain tissue had been routinely immersed in buffered 10% formalin for several weeks up to 6 months after which the wet tissue was archived in sealed plastic bags with a small excess of 10% formalin. Total fixation times varied from 4 months to 42 years. From a subset of subjects, several samples of the exact same brain had also been paraffin embedded at the beginning of their fixation process, normally within one month post-mortem. This allowed a direct comparison of structural changes with tissue from the same patients that was archived in formalin and embedded in paraffin several years later. (**Table 3.2**)

MRI

A slice of 20x15 mm brain tissue was selected from each subject and cut into a 4-mm-thick slice using a vibratome (VT1000S, Leica). The 4-mm slice was placed in a custom made tissue holder, immersed in a proton-free fluid (Fomblin, Solvay) and positioned in a vertical small-bore 9.4T Bruker Avance 400WB MRI system, equipped with a 1 T/m actively-shielded gradient insert and Paravision 4.0 imaging software (Bruker Biospin). A 20-mm birdcage transmit/receive coil was used (Bruker BioSpin). Several 3D T_2*-weighted gradient echo sequences were obtained with isotropic resolutions of 40 – 100 – 200 – 400 µm with the number of signal averages respectively being 60 – 20 – 20 – 12. TE/TR = 12.26 / 75 ms, FA = 25º. With the matrix size depending on the shape of each sample, average scan time per resolution were respectively 28 hrs, 2 hrs 40 min, 20 min. and 8 min. For quantitative T_2* measurements, 100 µm scans were also acquired using TE = 8 – 10 – 12.26 – 15 ms.

Histology

Following MRI, brain slices were paraffin-embedded and serially cut in 8-µm sections. Consecutive sections were stained for general microscopic morphology (hematoxylin and eosin (HE)), for myelin (Kluver-Barrera), for iron (Perls and a modified Perls DAB)[24] (FEIII-DAB, FEII-DAB)[25], copper (Romeis) and immunohistochemistry for Aβ (Dako, 6F/3D)[26], and GFAP (Dako, 6F2).[27] To allow correlation with MRI, sections were digitalized using a flatbed scanner (Agfa).

Electron microscopy

Electron microscopy was performed on a subset of subjects as previously described.[28] (**Table 3.2**) Collection was done on copper grids instead of carbon grids. Sections were examined using a JEOL JEM-1011 electron microscope operating at 60 kV and digitalized using a MegaView III camera.

Analysis / Scoring

Two sequential MR slices from the 3D data sets at 40 µm resolution were examined for "coarse" hypo-intensities defined by large size (120 – 1200 µm), irregular contour and

Table 3.1 Subject characteristics with corresponding macroscopic, MRI and histology scores

Subject nr.	Age / Sex (yr)	Post mortem pathologic evaluation	Fixation period (yr)	PMI (hrs)	Macroscopic discoloration	Coarse MR Hypo-intensities	Granular neuropil changes
1	88/F	AD	0.3		Absent	Absent	Absent
2	29/M	Control	0.3		Absent	Absent	Absent
3	70/F	sCAA	0.5		Absent	Absent	Absent
4	53/M	Control	0.5		Absent	Absent	Absent
5	53/M	Control	0.5		Absent	Absent	Absent
6	71/M	sCAA	0.5		Absent	Unknown	Absent
7	49/M	DS	1	13	Absent	Absent	Absent
8	64/M	AD	6	48	Present	Present	Present
9	58/M	HCHWA-D	6	6	Present	Present	Present
10	73/M	AD	7	9	Present	Present	Present
11	65/F	AD	7	2	Present	Extensive	Present
12	50/F	HCHWA-D	9	21	Present	Extensive	Extensive
13	45/F	HCHWA-D	15		Present	Extensive	Extensive
14	90/F	AD	16		Present	Extensive	Extensive
15	52/M	HCHWA-D	17	1	Present	Extensive	Extensive
16	62/F	DS	19		Present	Extensive	Extensive
17	62/M	Control	26		Present	Extensive	Extensive
18	58/F	AD	42	14	Present	Extensive	Extensive

M = Male; F = Female; sCAA = sporadic cerebral amyloid angiopathy; DS = Down's syndrome; AD = Alzheimer's disease; HCHWA-D = hereditary cerebral hemorrhage with amyloid Dutch type; PMI = Post-mortem interval; MRI coarse hypo-intensities: Absent = 0, Present = 1-10 hypo-intensities in one image, Extensive ≥ 10 hypo-intensities in at least one of the two examined images. Granular neuropil changes: Absent = 0, Present = 1-4 changes per section, Extensive ≥ 5 changes in at least 1 of the 3 sections.

elongated to stellate shape. These coarse hypo-intensities were scored as follows: absent: 0 coarse hypo-intensities, present: 1 – 9 coarse hypo-intensities, extensive: ≥10 coarse hypo-intensities. Three HE stained sections from the same level of the two sequential MRI slices were used to correlate MR images with histology. To perform these correlations, we used Adobe Photoshop 6.0 to visually overlay digitalized histological sections to their corresponding MR images. Of each patient the same HE sections were used to score the amount of granular neuropil changes as follows: "absent" if no granular neuropil changes were found, "present" for 1 – 4 and "extensive" for ≥ 5 neuropil changes in at least one out of the three sections.

Subjects with similar score were combined for group analysis (Mann-Whitney) to find significant differences (p-value < 0.05) in fixation period and age (SPSS 17).

pH of formalin

Of five patients with widely variable fixation times the pH of the formalin around the brain slices in sealed plastic bags, was determined using a logging pH meter (Hanna, H1 98230). (**Table 3.3**)

Table 3.2 Granular neuropil changes observed in brain tissue with short and long fixation times from within the same subject

Subject	Age / Sex (**yr**)	Post-mortem diagnosis	Granular neuropil changes Fixation period:	
			< 0.5 yr	9 - 42 yr
13	45/F	HCHWA-D	-	+
15	52/M	HCHWA-D	-	+
17	62/M	Control	-	+
18	58/F	AD	-	+

Table 3.3 pH-measurements

Subject	Post-mortem diagnosis	Fixation period (**yr**)	pH
5	Control	0.5	6.62
12	HCHWA-D	9	6.11
15	HCHWA-D	17	4.98
17	Control	26	5.43
18	AD	42	5.12
Fresh formalin			7

Results

MRI

High resolution T_2*-weighted images of eleven subjects showed irregularly contoured, elongated and stellate shaped hypo-intensities that were randomly distributed throughout the cortical gray matter and to a lesser degree in the white matter. (**Figure 3.1**) Their typical size (120 – 1200μm) and characteristic shape allowed clear distinction from possible other brain structures known to have a similar effect on T_2*, e.g. blood vessels or small roundish hypo-intensities caused by amyloid-β (Aβ) plaques, especially when including their spatial orientation. (**Figure 3.4**) Based on these characteristics, we defined them as "coarse hypo-intensities" and tissue was scored according to their presence. (**Table 3.1**)

When comparing similar MR images of the same section at decreasing resolution, these coarse hypo-intensities became less pronounced and harder to recognize as such. (**Figure 3.1**) This depended on their actual size and shape being affected by partial volume effects due to increasing voxel size. High and low resolution data were compared to assess if hypo-intense voxels on low resolution scans correlated with coarse hypo-intensities at high resolution. The largest coarse hypo-intensities were also visible at the lowest isotropic resolution of 400 μm, which is comparable to the *in vivo* MRI resolution. On quantitative T_2* maps, areas containing coarse hypo-intensities caused a clearly noticeable decrease in T_2*.

Pathology

Macroscopy

Only in brain tissue with coarse hypo-intensities on MRI, well circumscribed, white discolorations with similar size and distribution as the coarse MRI hypo-intensities were observed. (**Figure 3.2, Table 3.1**)

Histology

Microscopically, HE sections of tissue blocks with macroscopic white discolorations showed neuropil alterations with a close spatial correlation to the coarse MRI hypo-intensities. (**Figure 3.3** and **3.4**) These neuropil alterations comprised irregular, well circumscribed areas of granular, basophilic changes usually with some tissue rarefaction. (**Figure 3.5**) The corresponding Kluver's staining within these areas was decreased with respect to surrounding cortex/white matter suggesting a lower density of myelin. Most of these areas showed birefringence under polarized light in the HE that was not seen in unstained sections or the Kluver's stain that excludes the presence of anorganic material.

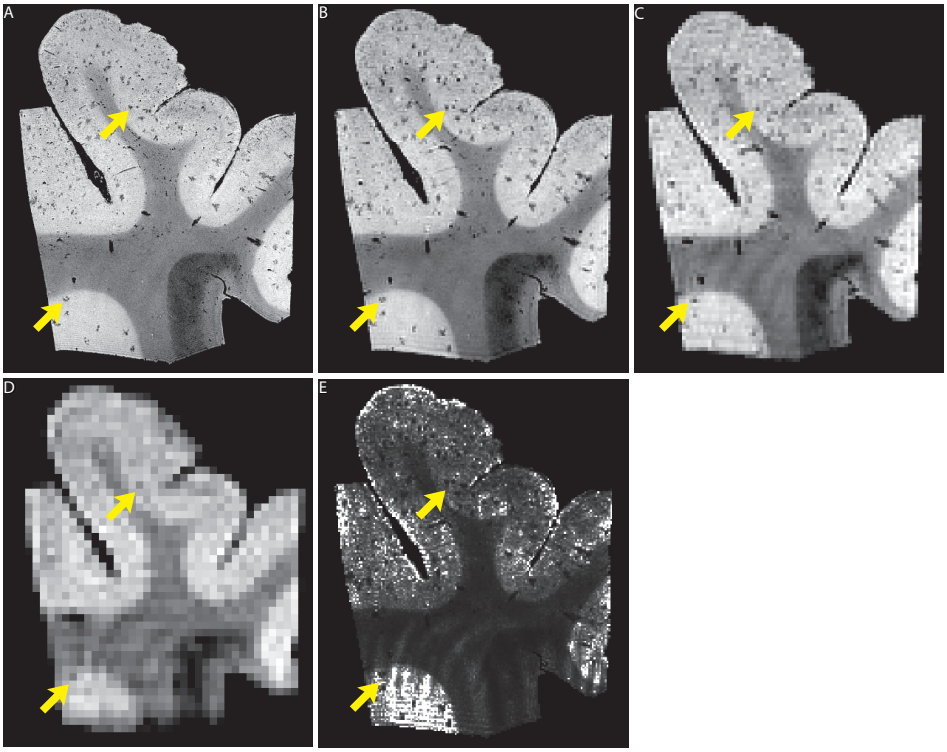

Figure 3.1 Hypo-intensities seen on MRI

Similar T_2*-weighted MR images of subject 14 acquired with isotropic resolution of respectively 40 µm (**A**), 100 µm (**B**), 200 µm (**C**) and 400 µm (**D**). Many coarse hypo intensities are detected in the higher resolution, but even at the lowest resolution (D) hypointense voxels are still discernible (*white arrows*). (**E**) shows the calculated T_2* map of the section in (B) with confirming a decreased T_2* relaxation.

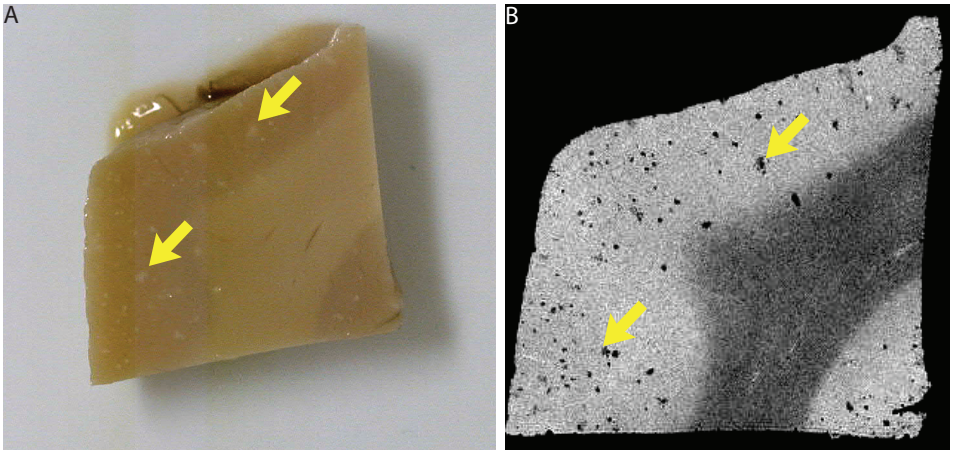

Figure 3.2 Macroscopic correlation
Images from subject 13 showing (**A**) fixated brain tissue with white discolorations (yellow arrows) and (**B**) high resolution (40 µm) T_2*-weighted MR images of the same brain tissue with coarse hypo intensities (*yellow arrows*).

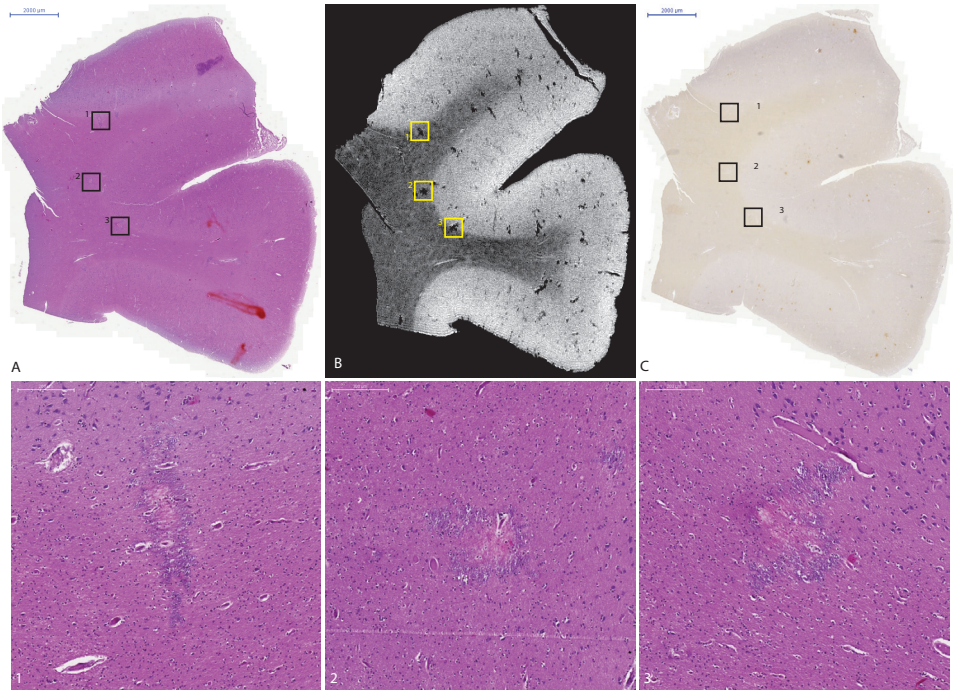

Figure 3.3 Histological correlation with MRI hypo-intensities of subject 17
Shown are the corresponding HE (**A**), MR image (**B**) and Aβ immunostained (**C**) sections of subject 17. Comparison of MR image with HE staining and Aβ staining correlating the granular neuropil changes with the The hypo-intensities seen on MRI correspond to areas of granular neuropil changes, as clearly depicted by the rectangular inserts (**1-3**) at 10x magnification. No Aβ deposition was observed at these locations.

The areas of basophilic granular neuropil changes were randomly distributed throughout the cortex and increasingly present in the white matter of tissue with long fixation times. These areas were found around vessels but also apart from vessels. The basophilic granular neuropil changes showed no signs of gliosis, hemorrhages or infarcts. Neurons, astrocytes, microglia and vessels were normally distributed within these areas and morphologically unaltered. Gemistocytes were not present. Furthermore, all histological (immuno)stainings for iron, copper and amyloid-β were negative within these areas. (**Figure 3.4**)
The basophilic granular neuropil changes were not only found in AD material but also in long fixated brain tissue of controls. In contrast, these changes were not found in short fixated AD material. Apart from the coarse hypo-intensities that co-localized with neuropil degeneration, other small roundish hypo-intensities were observed on MRI that did correspond to amyloid plaques. (**Figure 3.4**)

Electron microscopy
Tissue with macroscopic white discolorations showed localized areas with absent neuropil, although vessels were often present in these spaces on one-micron-thick, epoxy embedded tissue sections stained with toluidine blue. Electron microscopy of immediately adjacent ultrathin sections showed that these areas with absent neuropil actually consisted of spaces without any neuropil or only little neuropil remnants. (**Figure 3.6**) However, in these spaces varying amounts of lamellar structures were found, which were interpreted as membrane remnants and/or swollen degenerated myelin sheaths. Outside these circumscribed areas, we observed variable splitting and swelling of myelin sheets ranging from little splitting in otherwise normal myelin sheaths around axons, up to swollen myelin sheaths lining small empty spaces within the neuropil.

Relation of coarse MR hypo-intensities with fixation duration
The presence of coarse MR hypo-intensities, macroscopic and microscopic abnormalities were scored for each subject and the results are shown in **Table 3.1** Subjects with similar scores were combined for group analysis.
With regard to coarse MR hypo-intensities, fixation periods were significantly shorter when scored “absent” compared to “present” (p-value = 0.017 / r = -0.79). Furthermore, with even longer fixation periods, the number of hypo-intensities significantly increases when comparing “present” versus “extensive” (p-value = 0.018 / r = -0.71).
Similar results were obtained when comparing groups with different scores for granular neuropil changes. While fixation periods of those scored “absent” were significantly shorter as compared to those who were scored “present” (p-value = 0.006 / r = -0.82), which was significantly shorter as compared to “extensive” cases (p-value = 0.008 / r = -0.80).
No significant differences in subject’s age between groups were found for either coarse hypo intensity, histological or macroscopic score. Furthermore, no correlation was found between coarse MR hypo-intensities and presence/absence of disease regardless of type of disease.
In summary, brain tissue showed no changes when fixed for a period of one year or less in the same formalin solution, whereas changes were always present in tissue fixed for a period of 6 years or more tissue, and increasingly so with longer fixation periods.

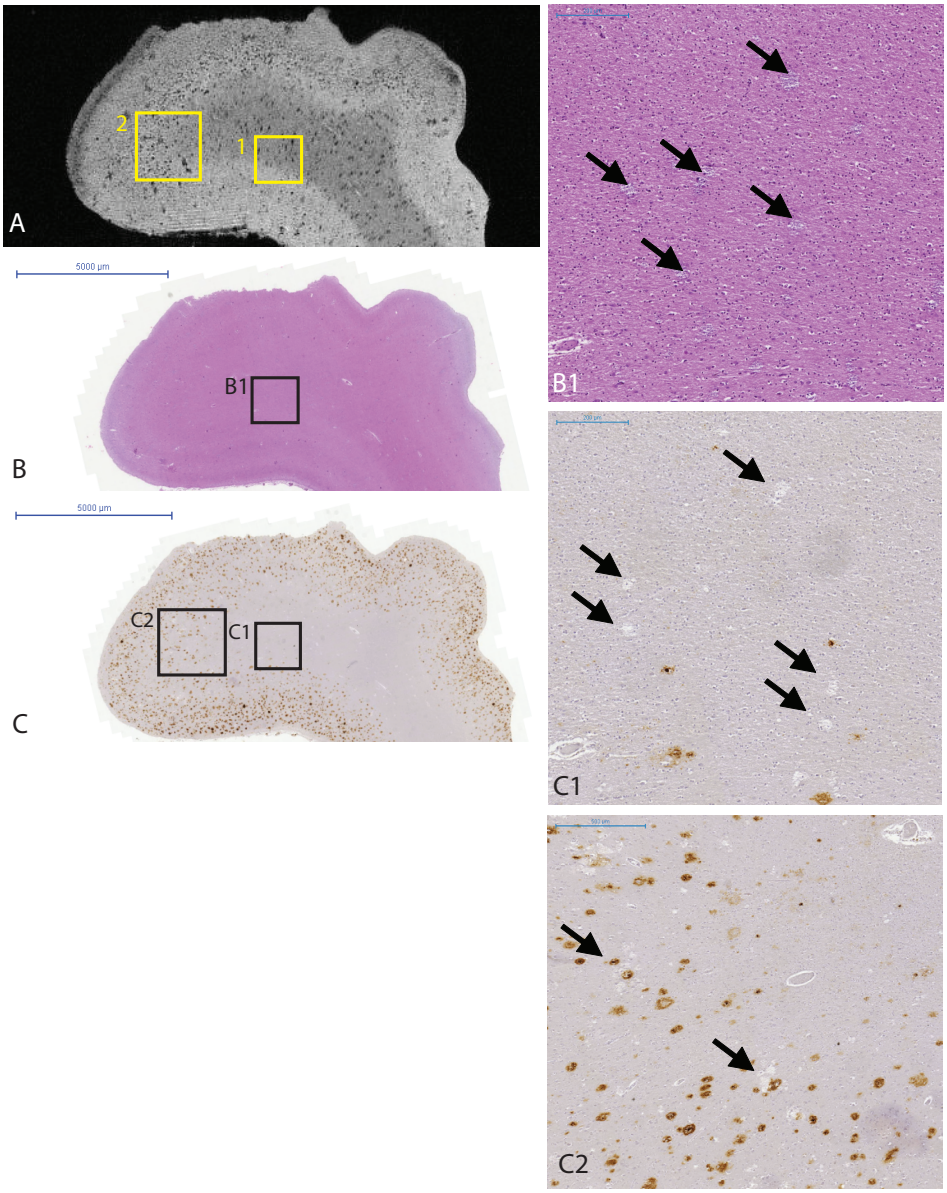

Figure 3.4 Another example of MRI hypo-intensities due to granular neuropil alterations
A MR image (**A**) of subject 18 is shown with its corresponding HE (**B**) and Aβ immunostaining (**C**). Granular neuropil changes in the white matter are observed without the presence of Aβ. (**B1**) represents the 10x magnification of the HE staining showing the granular neuropil changes in the white matter. The enlarged inserts (**C1** and **C2**, with respectively 10x and 5x magnifications) highlights that these changes in the WM are not depending on Aβ *as black arrows* highlight granular neuropil changes without Aβ (C1) and Aβ deposits with and without granular changes in the surrounding neuropil (C2).

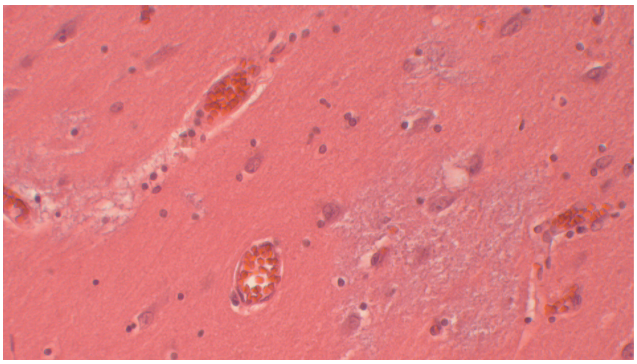

Figure 3.5 Detailed HE staining of the granular neuropil alterations (20x)

To test the hypothesis that prolonged formalin fixation indeed leads to histological and MR detectable changes, brain tissue from the same subject that was formalin fixed for either a short or a much longer period was compared microscopically. (**Table 3.2**) In the long-term fixed material, macroscopic white discolorations and granular neuropil changes were present, while short-term fixed material of the same subject completely lacked these findings, indeed supporting our hypothesis.
To obtain a complete picture, pH measurements were performed, because formalin solutions are known to become more acidic over time. pH measurements indeed showed increased acidity after longer periods of formalin fixation, as observed in the sealed plastic bags used for tissue storage. (**Table 3.3**)

Discussion and Conclusion

In the present study, "coarse hypo-intensities" on post-mortem brain MRI were seen corresponding to localized areas of neuropil destruction with remnants of membranes and myelin sheaths as observed by electron microscopy. These coarse hypo-intensities are mainly detected at high-resolution MR scans. Although brain tissue from Aβ-related diseases was used, the hypo-intensities where not related to deposits of iron, copper or Aβ correlating with these neurological diseases. Instead, these hypo-intensities appear to be an artifact associated with the duration of fixation within the same formalin. This can be concluded from the findings that these hypo-intensities were also detected in control tissue with long fixation times, and were not found in disease-related tissue fixated for a short period.
The exact mechanism of the described storage related artifacts is not known from previous studies but formalin solutions are known to become more acidic over time.[29] This was confirmed by pH measurements of the formalin excess around our sealed fixed brain tissue. Possibly neuropil destruction is caused by a local increase of acidity. However, continuous exposure to formalin and/or formic acid may form many other compounds that possibly play a role in causing artifactual tissue changes.[29,30] We were not able to study the effect of long term fixation in regularly refreshed formalin, and we can thus not exclude prolonged immersion in formalin itself as a cause of local neuropil destruction leading to

MR hypo-intensities rather than the increasing acidity or the formation of aggressive metabolites. Post-mortem autolysis does not appear to be the cause of the artifacts we have observed.

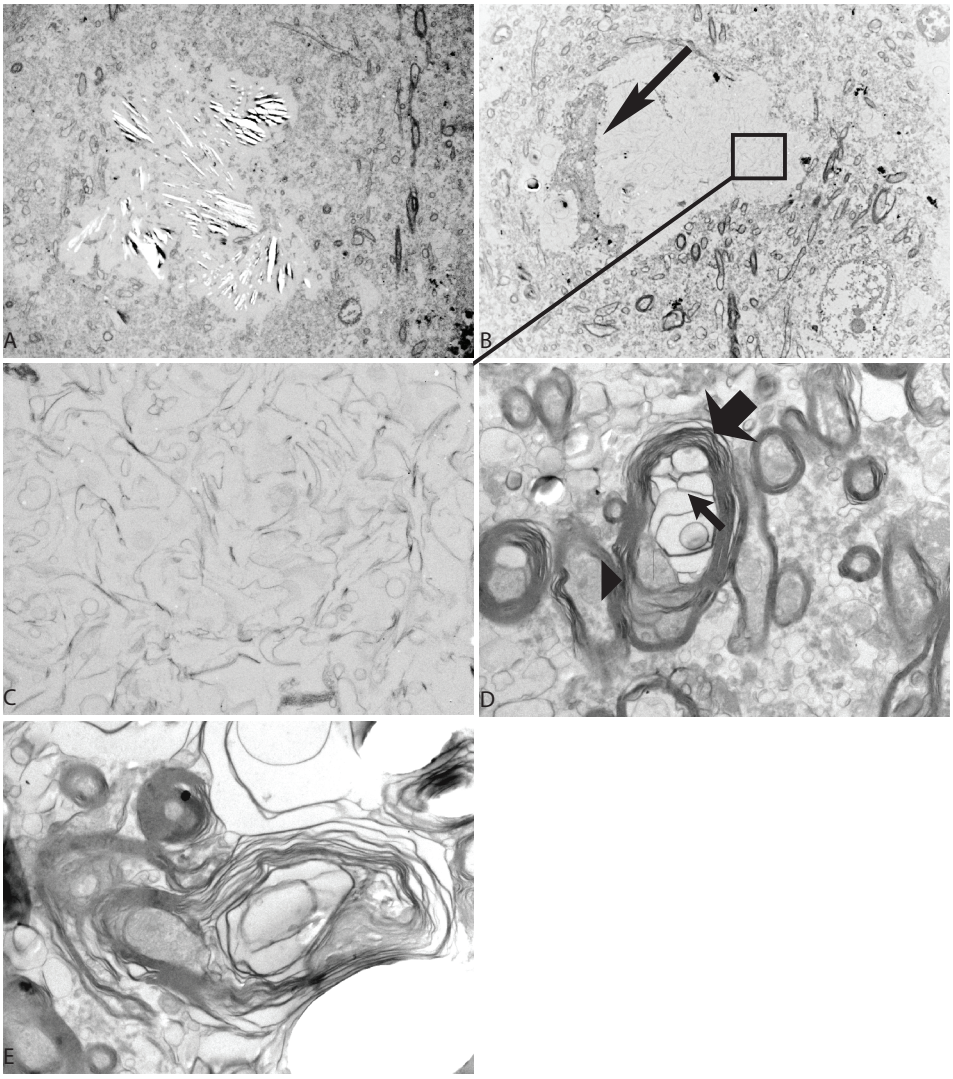

Figure 3.6 EM examination of the neuropil
Ultrastructure of localized areas of nearly empty spaces on semithin sections in long term formalin fixed tissue with macroscopic white discolorations. (**A**) These areas consisted of spaces without neuropil or only little neuropil remnants and often but not always contained a small blood vessel (1200x). (**B**) Circumscribed area of absent neuropil showing lamellar structures and a capillary (arrow) (1200x). (**C**) represents the lamellar structures in B (15000x). (**D**) shows myelinated axons, some with splitting of the myelin sheath. One axon (*arrowhead*) shows myelin splitting (*large arrow*) with little expansion of the spaces between the myelin sheaths (*small arrow*) (15000x). (E) A myelinated axon partly with intact myelin sheath and partly with myelin splitting with transition to more laminated structures with increasing spaces between the lamellae.

For this study, sufficient material fixed for a period of one to six years was lacking. Consequently, we can only conclude that neuropil artifacts occur in all tissue stored for a period of at least six years within the same formalin, whereas tissue stored for a period of one year or less showed no changes.

The coarse hypo-intensities correspond macroscopically to homogenous white discolorations in the tissue, and microscopically in 8 µm HE sections to granular neuropil alterations with slightly less density than the surrounding neuropil. The ultrathin sections (90 nm thick) used for EM revealed that these areas represented absent neuropil with partial filling of the resulting spaces by membrane-like structures. We speculate that this degenerated membraneous/proteineous material with weak birefringence causes hypo-intensities on MRI due to its solid-state-like properties.

The low signal intensity on MRI may also result from replacement of formalin solution by proton free fluid in these relatively more empty spaces. However, a decrease in proton density would not cause a T_2* decrease, as was observed in the T_2* maps.

With respect to the induced MR changes, previous reports state that formalin fixation causes changes in relaxation and diffusion properties, thereby altering MR contrast, even though the exact mechanism remains unclear.[16] These changes in MR properties, however, occur throughout the entire sample and are partially reversible by rehydrating the sample in PBS. In contrast, the structural disruptions we found after prolonged formalin fixation are very localized and irreversible. Detected changes were furthermore not related to any of the known possible changes due to prolonged PMI as described elsewhere.[13,15,17,20,21] For this study brain tissue of all kinds of PMI periods was used, and no correlation was found with either the tissue changes or MRI hypo-intensities. (**Table 3.1**)

The conclusion of this study suggests that data of several earlier published studies, using post-mortem brain tissue of patients with Alzheimer's disease (AD) for MRI [1-12], should be cautiously interpret. In these studies, hypo-intense spots were observed on T_2*- or T_2-weighted scans that co-localised with dense amyloid plaques and iron accumulations.[1-12] However, brain tissue in these studies was collected within a short period, and fixed for a maximum period of a few months.

With regard to the detection of amyloid plaques, we also observed hypo-intense spots on MRI that corresponded to the presence of amyloid plaques. However, these did not correlate with the larger stellar shape coarse hypo-intensities. (**Figure 3.4**) The possible Aβ plaque detection indicates that the basic mechanisms for MR contrast (iron accumulation, dense protein aggregates) are still present. On ultra-high resolution scans, these different hypo-intensities can be easily distinguished. However, on scans with a lower resolution, e.g. those comparable to resolutions that can be achieved on clinical MRI systems, both forms might become indistinguishable, and based upon their size the coarse hypo-intensities due to fixation artifacts are more likely to remain visible. (**Figure 3.1**) In our study, these low resolution images were acquired at relatively short echo times; when a stronger T_2*-weighting would be used, more hypo-intensities would be observable at these lower resolutions. Furthermore, it is important to realise that although these neuropil changes are beyond the anatomical resolution of scans with clinical resolutions, they could still be visible on such scans because their signal differs so strongly from surrounding tissue.

Other known sources for hypo-intensities on T_2*-weighted images, like calcifications, iron deposits, microbleeds or cavernous malformations[31] could be easily disregarded within this study, while their presence could not be confirmed upon histology. However, especially when conducting similar *ex vivo* MR studies for either one of these pathologies using old brain material and clinically relevant resolutions, one should be aware that the described formalin fixation artifacts could possibly lead to similar hypo-intensities and thus a misinterpretation of the data.
In order to put our findings into a broader perspective, a small survey was conducted among eight other brain banks and neuropathology departments regarding their brain storage protocol. Three of these centers store their formalin-fixed brain tissue in sealed plastic bags with little excess formalin similar to the tissue used in this study, whereas four other centers store fixed brain tissue floating in formalin, two without a protocol for regularly refreshing it, one renewing formalin "when necessary" and the fourth every few years. The last center stores brains in polyethyleenglycol. How the different storage protocols affect the general tissue quality with respect to *ex vivo* MRI research after long term storage remains to be further investigated, but this small survey shows that the fixation protocol for our study is common practice among brain banks, and therefore the findings will have implications for future research on brain bank tissue.

In conclusion, our results demonstrate that fixed brain tissue stored for prolonged periods gives rise to structural tissue changes that are associated with hypo-intensities on T_2*-weighted MR images. When brain tissue from pathology archives or brain banks is used to study (rare) disorders with *ex vivo* MRI, it is of vital importance to take the storage protocol into account and to check for the macroscopic and microscopic alterations that have been described and illustrated in this study.

References

1. Benveniste, H, Einstein, G, Kim, KR, *et al*. Detection of neuritic plaques in Alzheimer's disease by magnetic resonance microscopy. Proc Natl Acad Sci U S A. 1999; 96:14079-14084.
2. Bobinski, M, de Leon, MJ, Wegiel, J, *et al*. The histological validation of post mortem magnetic resonance imaging-determined hippocampal volume in Alzheimer's disease. Neuroscience. 2000; 95:721-725.
3. Bronge, L, Bogdanovic, N, and Wahlund, LO. Post-mortem MRI and histopathology of white matter changes in Alzheimer brains. A quantitative, comparative study. Dement Geriatr Cogn Disord. 2002; 13:205-212.
4. Englund, E, Sjobeck, M, Brockstedt, S, *et al*. Diffusion tensor MRI post mortem demonstrated cerebral white matter pathology. J Neurol. 2004; 251:350-352.
5. Fernando, MS, O'Brien, JT, Perry, RH, *et al*. Comparison of the pathology of cerebral white matter with post-mortem magnetic resonance imaging (MRI) in the elderly brain. Neuropathol Appl Neurobiol. 2004; 30:385-395.
6. Geurts, JJ, Bo, L, Pouwels, PJ, *et al*. Cortical lesions in multiple sclerosis: combined post-mortem MR imaging and histopathology. AJNR Am J Neuroradiol. 2005; 26:572-577.
7. Gouw, AA, Seewann, A, Vrenken, H, *et al*. Heterogeneity of white matter hyperintensities in Alzheimer's disease: post-mortem quantitative MRI and neuropathology. Brain. 2008; 131:3286-3298.
8. House, MJ, St Pierre, TG, Kowdley, KV, *et al*. Correlation of proton transverse relaxation rates (R2) with iron concentrations in post-mortem brain tissue from alzheimer's disease patients. Magn Reson Med. 2007; 57:172-180.
9. Kangarlu, A, Bourekas, EC, Ray-Chaudhury, A, *et al*. Cerebral cortical lesions in multiple sclerosis detected by MR imaging at 8 Tesla. AJNR Am J Neuroradiol. 2007; 28:262-266.
10. Larsson, EM, Englund, E, Sjobeck, M, *et al*. MRI with diffusion tensor imaging post-mortem at 3.0 T in a patient with frontotemporal dementia. Dement Geriatr Cogn Disord. 2004; 17:316-319.
11. Schmierer, K, Parkes, HG, So, PW, *et al*. High field (9.4 Tesla) magnetic resonance imaging of cortical grey matter lesions in multiple sclerosis. Brain. 2010; 133:858-867.
12. van Rooden, S, Maat-Schieman, ML, Nabuurs, RJ, *et al*. Cerebral amyloidosis: post-mortem detection with human 7.0-T MR imaging system. Radiology. 2009; 253:788-796.
13. Blamire, AM, Rowe, JG, Styles, P, *et al*. Optimising imaging parameters for post mortem MR imaging of the human brain. Acta Radiol. 1999; 40:593-597.
14. Dawe, RJ, Bennett, DA, Schneider, JA, *et al*. Post-mortem MRI of human brain hemispheres: T2 relaxation times during formaldehyde fixation. Magn Reson Med. 2009; 61:810-818.
15. Pfefferbaum, A, Sullivan, EV, Adalsteinsson, E, *et al*. Post-mortem MR imaging of formalin-fixed human brain. Neuroimage. 2004; 21:1585-1595.
16. Shepherd, TM, Thelwall, PE, Stanisz, GJ, *et al*. Aldehyde fixative solutions alter the water relaxation and diffusion properties of nervous tissue. Magn Reson Med. 2009; 62:26-34.
17. Shepherd, TM, Flint, JJ, Thelwall, PE, *et al*. Post-mortem interval alters the water relaxation and diffusion properties of rat nervous tissue--implications for MRI studies of human autopsy samples. Neuroimage. 2009; 44:820-826.
18. Tovi, M and Ericsson, A. Measurements of T1 and T2 over time in formalin-fixed human whole-brain specimens. Acta Radiol. 1992; 33:400-404.
19. Yong-Hing, CJ, Obenaus, A, Stryker, R, *et al*. Magnetic resonance imaging and mathematical modeling of progressive formalin fixation of the human brain. Magn Reson Med. 2005; 54:324-332.
20. Nagara, H, Inoue, T, Koga, T, *et al*. Formalin fixed brains are useful for magnetic resonance imaging (MRI) study. J Neurol Sci. 1987; 81:67-77.
21. D'Arceuil, HE, Westmoreland, S, and de Crespigny, AJ. An approach to high resolution diffusion tensor imaging in fixed primate brain. Neuroimage. 2007; 35:553-565.
22. Metz, B, Kersten, GF, Hoogerhout, P, *et al*. Identification of formaldehyde-induced modifications in proteins: reactions with model peptides. J Biol Chem. 2004; 279:6235-6243.
23. Puchtler, H and Meloan, SN. On the chemistry of formaldehyde fixation and its effects on immunohistochemical reactions. Histochemistry. 1985; 82:201-204.
24. LeVine, SM. Oligodendrocytes and myelin sheaths in normal, quaking and shiverer brains are enriched in iron. J Neurosci Res. 1991; 29:413-419.
25. Smith, MA, Harris, PL, Sayre, LM, *et al*. Iron accumulation in Alzheimer disease is a source of redox-generated free radicals. Proc Natl Acad Sci U S A. 1997; 94:9866-9868.

26. Natte, R, Maat-Schieman, ML, Haan, J, *et al*. Dementia in hereditary cerebral hemorrhage with amyloidosis-Dutch type is associated with cerebral amyloid angiopathy but is independent of plaques and neurofibrillary tangles. Ann Neurol. 2001; 50:765-772.
27. Viale, G, Gambacorta, M, Coggi, G, *et al*. Glial fibrillary acidic protein immunoreactivity in normal and diseased human breast. Virchows Arch A Pathol Anat Histopathol. 1991; 418:339-348.
28. Natte, R, Yamaguchi, H, Maat-Schieman, ML, *et al*. Ultrastructural evidence of early non-fibrillar Abeta42 in the capillary basement membrane of patients with hereditary cerebral hemorrhage with amyloidosis, Dutch type. Acta Neuropathol. 1999; 98:577-582.
29. Matubayasi, N and Nakahara, M. Hydrothermal reactions of formaldehyde and formic acid: free-energy analysis of equilibrium. J Chem Phys. 2005; 122:074509.
30. Schrag, M, Dickson, A, Jiffry, A, *et al*. The effect of formalin fixation on the levels of brain transition metals in archived samples. Biometals. 2010.
31. Greenberg, SM, Vernooij, MW, Cordonnier, C, *et al*. Cerebral microbleeds: a guide to detection and interpretation. Lancet Neurol. 2009; 8:165-174.

PART ONE | Native MRI contrast

1 Department of Radiology, C.J. Gorter Center for High Field MRI, Leiden University Medical Center, Leiden, The Netherlands
2 Department of Anatomy & Embryology, Leiden University Medical Center, Leiden, The Netherlands
3 Department of Neurology, Leiden University Medical Center, Leiden, The Netherlands
4 Department of Pathology, Leiden University Medical Center, Leiden, The Netherlands
5 Molecular Imaging Laboratories Leiden, MRI Lab, Leiden University Medical Center, Leiden, The Netherlands